Atmospheric Chemistry and Physics Discussions

The UV-visible absorption cross-sections of IONO$_2$

J. C. Mössinger[1], D. M. Rowley[1,2], and R. A. Cox[1]

[1]Centre for Atmospheric Science, Chemistry Department, University of Cambridge, UK
[2]Present address Chemistry Department, University College London, UK

Correspondence to: J. C. Mössinger (jcm34@hermes.cam.ac,uk)

The IONO$_2$ absorption cross-sections

J. C. Mössinger et al.

Abstract

The UV-visible absorption spectrum of gaseous IONO$_2$ has been measured over the wavelength range 245–415 nm using the technique of laser photolysis with time-resolved UV-visible absorption spectroscopy. IONO$_2$ was produced in situ in the gas phase by laser flash photolysis of NO$_2$/CF$_3$I/N$_2$ mixtures. Post-flash spectra were deconvolved to remove contributions to the observed absorption from other reactant and product species. The resulting spectrum attributed to IONO$_2$ consists of several overlapping broad absorption bands. Assuming a quantum yield of unity for IONO$_2$ photolysis, model calculations show that during sunlit hours at noon, 53° N, the first order solar photolysis rate coefficient (J value) for IONO$_2$ is $4.6 \times 10^{-2}\,\text{s}^{-1}$.

1. Introduction

Iodine chemistry has been implicated in tropospheric ozone depletion since the 1980s (Chameides and Davis, 1980; Davis et al., 1996; Jenkin et al., 1985). Atmospheric iodine source gases are readily photolysed by sunlight, yielding iodine atoms. Iodine atoms react with ozone forming IO. Any subsequent reactions of IO forming an iodine atom lead to catalytic ozone loss. In competition, IO can be sequestered into reservoir species. One of the main gaseous reservoir species for iodine in the atmosphere is believed to be IONO$_2$ (Chameides and Davis, 1980; Davis et al., 1996; Jenkin, 1992; Jenkin et al., 1985).

IONO$_2$ is formed by the reaction of IO with NO$_2$

$$\text{IO} + \text{NO}_2 + \text{M} \rightarrow \text{IONO}_2 + \text{M} \tag{R1}$$

The rate of formation of IONO$_2$ in reaction (1) is well known (De More et al., 1997) but the amount of IONO$_2$ residing in the atmosphere and its consequent impact on the atmospheric chemistry depends on its loss processes. Gas phase IONO$_2$ loss processes include photolysis, thermal decomposition and heterogeneous uptake.

IONO$_2$ can be photolysed via two possible routes:

$$IONO_2 + h\nu \rightarrow IO + NO_2 \hspace{4cm} \text{(R2a)}$$

$$\rightarrow I + NO_3 \hspace{4cm} \text{(R2b)}$$

However, no studies of the absorption cross-sections, the photolysis quantum yields
or the products of IONO$_2$ photolysis have been reported to date.

Thermal decomposition of IONO$_2$ could proceed as in reaction (3).

$$IONO_2 \xrightarrow{\Delta} IO + NO_2 \hspace{4cm} \text{(R3)}$$
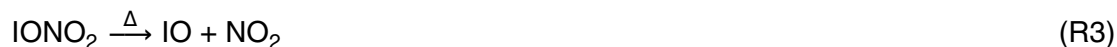
However, recent observations imply that reaction (3) is a slow process at ambient temperature (Dillon, 2001; Plane, 2002).

A recent study has provided the first experimental evidence that IONO$_2$ can be lost from the gas phase *via* a heterogeneous process. In a laboratory study, Holmes et al. (2001) showed that IONO$_2$ is taken up efficiently by dry and frozen salt surfaces to form the di-halogens IBr and ICl, which are then released back into the gas phase.

IONO$_2$ has been synthesised in the laboratory in solution. However, IONO$_2$ was found to be unstable and the first attempts to observe its ultraviolet-visible absorption spectrum failed (Schmeisser and Braendle, 1961). The absorption cross-sections for IONO$_2$ in the UV-visible are essential, in order to evaluate the daytime atmospheric photolysis rate of IONO$_2$ and the efficiency of the tropospheric ozone loss cycle involving IONO$_2$.

Broske and Zabel (1998) attempted to measure the gas phase UV-visible absorption spectrum of IONO$_2$ by photolysis of I$_2$/NO$_2$ mixtures in a large reaction chamber equipped for in situ spectroscopy. A diode array detector was used to monitor the UV-visible absorption spectrum. However, because of the low concentrations of IONO$_2$ produced under their experimental conditions and the presence of strong absorbers such as INO$_2$, produced by the reaction of iodine atoms produced from I$_2$ photolysis with NO$_2$, they were unable to retrieve the spectrum of IONO$_2$. Nevertheless, the UV-visible absorption spectrum of gaseous INO$_2$ was reported (Atkinson et al., 2000).

© EGS 2002

In order to avoid the effects of complicating chemistry involving iodine atoms produced in the IO source reactions, as well as the effects of secondary chemistry, a pulsed laser photolysis system and a photochemical source of IO with no initial iodine atom production (NO_2/CF_3I) was used in this study. We report here, for the first time

5 observation of a gas phase ultraviolet-visible spectrum attributed to $IONO_2$. The results were used to calculate the atmospheric photolysis rates of $IONO_2$, and the atmospheric chemistry of $IONO_2$ is discussed briefly.
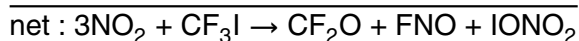
2. Experimental

The $IONO_2$ absorption spectrum was obtained using the technique of laser flash pho-
10 tolysis with UV absorption spectroscopy, utilising a CCD detection system. The apparatus has been described in detail elsewhere (Rowley et al., 1996), therefore only a brief description is given here.

During an experiment gases were flowed slowly and continuously through a 98.2 cm long cylindrical quartz cell kept at a total pressure of 760 Torr. Reactions were
15 initiated in the cell using a pulsed excimer laser beam passed longitudinally along the cell. Concentrations of reactant and product gases in the cell were monitored using UV-vis absorption spectroscopy. The analysis light beam from a xenon arc lamp was passed through the cell, counter propagating the laser beam, and focused onto the entrance slit of a 0.25 m focal length astigmatic Czerny-Turner spectrograph fitted with
20 three interchangeable diffraction gratings ruled at 150, 300 and 600 grooves/mm. In order to protect the spectrograph and detector from impinging reflected laser light a narrow band filter was used in the 350 nm region. Wavelength resolved analysis light from the spectrograph was then imaged across the top 30 rows of a CCD detector, to record spectra. Signal (charge) transfer then enabled recording of sequential spectra,
25 which were acquired before, during and after photolysis.

A $NO_2/CF_3I/N_2$ chemical system was employed to generate $IONO_2$ via the following

reaction scheme:

$$NO_2 + h\nu \rightarrow NO + O(^3P) \tag{R4}$$

$$O(^3P) + CF_3I \rightarrow CF_3 + IO \tag{R5}$$

$$IO + NO_2 + M \rightarrow IONO_2 + M \tag{R1}$$

5 $$CF_3 + NO_2 \rightarrow CF_2O + FNO \tag{R6}$$

net : $3NO_2 + CF_3I \rightarrow CF_2O + FNO + IONO_2$

The reaction was initiated using 351 nm XeF excimer laser photolysis of NO_2 to form $O(^3P)$ (DeMore et al., 1997). N_2 (Messer, 99.996%), 2000 ppm NO_2 in N_2 (Messer) and CF_3I (Fluorochem, 99%) were used as supplied. Gas mixtures were flowed through the
10 reaction cell at a total pressure of 760 Torr and at 298 K via mass flow controllers or ball flow meters (for NO_2 in N_2) and their concentrations (see Table 1 for concentrations used) were calculated from known calibrated flow rates. Postflash absorbance spectra were recorded relative to preflash spectra using Beer's law ($A = \ln(I_{preflash}/I_{postflash})$). Consequently, the observed absorbances show changes in absorption brought about
15 by the laser flash and by subsequent chemistry. The total absorption spectrum of the gas mixture was recorded using a 150 g/mm and a 300g/mm grating giving a 130 nm and a 65 nm wavelength coverage respectively. In the 245–335 nm region the 150g/mm grating was used with a 50 μm spectrograph entrance slit giving a resolution (fwhm) of 1.67 nm. In the 385–415 nm region the 300g/mm grating was used with a 10
20 μm entrance slit and a resolution (fwhm) of 0.55 nm. In both cases a CCD was used to record sequential spectra at a time resolution of 1 ms.

Under the conditions chosen (Table 1) numerical models show that the chemistry of IO and CF_3 dominates, as $O(^3P)$ reacts mainly (93%) with CF_3I. In addition, only small amounts of NO are expected (from NO_2 photolysis and the $O(^3P) + NO_2$ reaction (7%))

and I atom production from the reaction IO + NO → I + NO$_2$ is consequently unimportant. Thus, the possible formation of INO$_2$ via reaction I + NO$_2$ + M → INO$_2$ + M is unlikely. IONO$_2$ is expected to be the only major iodine containing product formed under the experimental conditions used, as the reaction of NO$_2$ with IO dominates over other

5 possible reactions with IO. Thus, the IONO$_2$ spectrum can in principle be obtained from the experimental spectrum, after subtraction of the absorption due to CF$_2$O and FNO formed via reaction (6) and addition of absorbance due to NO$_2$ and CF$_3$I consumed in reactions (4) and (5), respectively. However, it should be noted that the yield for reaction (5) is 0.85 (Gilles et al., 1996). The identity of the remaining reaction channels

10 is unknown (Gilles et al., 1996). Other products that could be formed via reaction (5) such as IF or CF$_3$IO could also contribute to the overall absorption spectrum obtained. However, since their absorption cross-sections have not been reported to date it is not possible to correct for their contribution to the overall absorption. Thus an uncertainty of ± 15% remains in the IONO$_2$ spectrum determined. Other secondary and side re-

15 actions that occur were taken into account by using the numerical integration package FACSIMILE (Curtis and Sweetenham, 1987) to model the post flash chemistry in order to calculate the final product distribution. Details of the chemical reaction scheme used are listed in Table 2. Spectra were not recorded below 245 nm or between 335–385 nm, due to low light levels of the analysis light beam in these regions, the latter due to

20 the attenuation by the laser beam filter in the 350 nm region. The overall error on the IONO$_2$ absorption cross-sections including the uncertainty due to the unknown reaction channels mentioned above is 25%. This excludes possible systematic errors that could result from the chemical mechanism used in the FACSIMILE model.

3. Results and discussion

25 The absorption spectrum recorded in the short wavelength region (245–345 nm) of the spectrum (Fig. 1), i.e. the absorbance calculated relative to pre-laser intensities, represents the change in absorption due to the overall chemical reaction initiated by

the laser flash. In the analysis it was assumed that only the 5 principal species (NO_2, CF_3I, FNO, CF_2O and $IONO_2$) contribute to this absorption. Thus a negative change in absorption results from NO_2 and CF_3I consumption and a positive change in absorption due to $IONO_2$, CF_2O and FNO production make up the observed spectrum. The post

5 flash spectrum obtained was reproducible and remained constant over the time-scale of the spectral acquisition (the photolysed gas flowed out of the cell over a period of 10–15 s). The total absorption spectrum measured and the absorption spectrum of $IONO_2$ can be expressed as shown in Eq. (1) and (2), respectively.

$$A_{total} = A_{IONO_2} + A_{CF_2O} + A_{FNO} - A_{NO_2} - A_{CF_3I} \tag{1}$$

10 $$A_{IONO_2} = A_{total} - A_{CF_2O} - A_{FNO} + A_{NO_2} + A_{CF_3I} \tag{2}$$

Thus, $IONO_2$ was found by spectral deconvolution. The contribution of each absorber to the total absorption at each wavelength recorded during an experiment is given by:

$$A(\lambda) = \sigma_i(\lambda) \times l \times \Delta c_i \tag{3}$$

15 where $A(\lambda)$ is the absorbance of a species i at wavelength λ, l is the pathlength of the reaction cell used [cm], Δc = change in concentration of species i [molecules cm^{-3}] and $\sigma_i(\lambda)$ = absorption cross-section of species i at that wavelength [$molecule^{-1}$ cm^2].

In order to obtain the $IONO_2$ spectrum the amounts and the absorption cross-sections of all other chemical species involved have to be known.

20 The absolute cross-sections of CF_3I, FNO and CF_2O have been reported in the literature (DeMore et al., 1997) and were smoothed to the spectral resolution used for the present experiment (CF_2O only absorbs at wavelength shorter than 245 nm and its contribution to the overall absorption is thus not shown in Fig. 2). The change in concentration of each species after the laser flash is determined by the O atom concentration

25 produced from NO_2 photolysis in the flash and the stoichiometry of subsequent chemistry. In order to determine these concentration changes a kinetic model of the reaction

J. C. Mössinger et al.

system was constructed in the numerical integration package FACSIMILE (Curtis and Sweetenham, 1987). The model incorporated simulations of photolysis, flow out and the chemical reaction scheme given in Table 2. The model provided the simulated change in concentration of each species during an experiment for all given experimental conditions with the initial post flash O atom concentration being the only variable. The initial O atom concentration was determined from the change in NO$_2$ concentration in any given experiment, which itself was obtained from the measured initial change in absorption of NO$_2$ and its cross-section. Together with the known cross-sections, the contribution of each species to the absorption spectra was then subtracted from the overall post flash spectrum recorded as shown in Fig. 2 for the 245–335 nm region of the spectrum. The absorption cross-sections of IONO$_2$ were then obtained assuming the remaining absorption was attributed to the simulated amount of IONO$_2$ generated in the reaction. The same procedure was also applied to the data obtained in the longer wavelength region (385–415 nm) as shown in Fig. 3. However, in this wavelength region only NO$_2$ absorbs significantly and thus the NO$_2$ spectrum had to be subtracted from the total absorption spectrum. The IONO$_2$ absorption spectrum over the entire wavelength range of 245–415 nm was obtained by fitting the observed spectrum to three Gaussian functions. This enabled interpolation of the IONO$_2$ absorption in spectral regions where absorbance could not be recorded. The resulting spectrum consists of a broad continuous absorption band as shown in Fig. 4. The IONO$_2$ cross-sections are listed in Table 3. The fact that the structural features of FNO and NO$_2$ do not appear to a significant extent in the final spectrum provides support for the deconvolution procedure used. The IONO$_2$ absorption spectrum obtained is compared in Fig. 5 to the INO$_2$ spectrum (Atkinson et al., 2000). It is distinctly different, supporting the assignment to IONO$_2$. There is also a possibility of a contribution to the apparent IONO$_2$ spectrum from formation of light scattering aerosol produced in the IO radical chemistry. A maximum potential contribution to the absorption from aerosol was calculated assuming all absorption at λ = 450 nm was due to aerosol extinction and that the attenuation at lower wavelength followed a $1/\lambda^4$ functional dependence on wavelength.

After subtraction of this component the lower curve in Fig. 5 was obtained which corresponds to minimum values for the IONO$_2$ cross-sections. Examination of time resolved absorption spectra also show no evidence for time delayed aerosol growth for the first two experiments performed in a clean flow tube. After rapid formation of IONO$_2$ the

5　absorption remained constant over the whole time period of the experiment (500 ms). Only after multiple experiments in the flow tube did we observe a time delayed increase in overall absorption with time, possibly due to the presence of aerosols, presumably formed in heterogeneous processes initiated on the walls of the reaction cell.

　　Figure 6 shows a comparison of the IONO$_2$ absorption and the (IONO$_2$-aerosol)

10　absorption with those of ClONO$_2$ (Burkholder et al., 1994) and BrONO$_2$ (Burkholder et al., 1995). All spectra show similar broad band absorption features. The absorption due to IONO$_2$ is red shifted and is significantly more intense at all wavelengths than the chlorine and bromine analogues.

4. Atmospheric implications

15　The IONO$_2$ absorption cross-sections recorded here were used to calculate the tropospheric solar photolysis rate of IONO$_2$ using a photochemical box model (McFiggans et al., 2000). We assumed a quantum yield of unity for IONO$_2$ photolysis throughout the absorption band. The resulting photolysis rate coefficient (J-value) for IONO$_2$ is shown in Fig. 7 as a function of time of day in the marine boundary layer, for July 53° N at Mace

20　Head, Ireland, where measurements of atmospheric composition had taken place in 1997. The calculated photolytic lifetime of IONO$_2$ under these conditions is less than one minute. At the same location and time, the surface to volume ratio (S/V) of the fine fraction of the sea-salt aerosol present was determined to be 60 ± 10 μm^2 cm^{-3} with an effective particle radius of 250 nm (McFiggans et al., 2000). Using these values,

25　the lifetime of IONO$_2$ with respect to heterogeneous uptake on sea-salt aerosols, τ_{het} [s], was calculated to be $\sim$ 10 h using Eqs. (4) and (5) below, and assuming a reactive uptake coefficient of γ = 0.01 (Holmes et al., 2001). Equation (4) assumes spherical

geometry of the sea-salt particle. It also takes diffusion of $IONO_2$ to the particle surface into account (Turco et al., 1989).
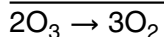
$$k_{het} = \frac{0.25 \times \gamma \times \omega \times S/V}{(1 + (3 \times \gamma \times r)/(4 \times \lambda))} \qquad (4)$$

$$\tau_{het} = \frac{1}{k_{het}} \qquad (5)$$

5   where ω = the average molecular speed of $IONO_2$ at any given temperature [cm s^{-1}], k_{het} = first order rate constant for loss of $IONO_2$ on the aerosol [s^{-1}], λ = mean free path of a molecule in air at any given temperature and pressure [cm].

    During daytime, solar photolysis is thus expected to be the major loss process for $IONO_2$ and IO_x is not lost from the gas phase. However, the reaction of $IONO_2$ with
10 sea-salt aerosol may become a significant loss process for $IONO_2$ during night time. Uptake of $IONO_2$ is expected to form the di-halogens ICl and IBr (Holmes et al., 2001), which are released into the gas phase during the night. At dawn, IBr and ICl are photolysed. Hence IO_x would not be lost permanently from the gas phase via this reaction as suggested previously (Chatfield and Crutzen, 1990; Davis et al., 1996; Jenkin, 1992),
15 and the uptake of $IONO_2$ represents a possible route to liberation of bromide and chloride from sea-salt aerosols, as has been predicted by more recent modelling studies (McFiggans et al., 2000; Vogt et al., 1999). Thermal decomposition of $IONO_2$ may also contribute to the night time loss of $IONO_2$. However, recent observations seem to suggest that this will be a very slow process at room temperature (Plane, 2002).
20 Depending upon the photolysis product yields, photolysis of $IONO_2$ could contribute directly to ozone destruction via the following reaction cycle:

$$IO + NO_2 + M \rightarrow IONO_2 + M \tag{R1}$$

$$IONO_2 + h\nu \rightarrow I + NO_3 \tag{R2b}$$

$$NO_3 + h\nu \rightarrow NO + O_2 \tag{R7}$$

$$NO + O_3 \rightarrow NO_2 + O_2 \tag{R8}$$

$$I + O_3 \rightarrow IO + O_2 \tag{R9}$$

$$\overline{2O_3 \rightarrow 3O_2}$$

However, it is important to note, that this cycle will not operate if the products of $IONO_2$ photolysis are $IO + NO_2$. No studies of the photolysis products of $IONO_2$ have been reported, and such studies are essential to elucidate further the role of atmospheric $IONO_2$.

5. Conclusions

The UV-visible cross-sections of $IONO_2$ have been determined over the wavelength ranges 240–335 nm and 385–415 nm Both data sets were used to interpolate an $IONO_2$ absorption spectrum over the wavelength range of 240–415 nm. The resulting spectrum consists of several overlapping broad absorption bands. Based on the $IONO_2$ absorption cross-section, the tropospheric solar photolysis rate coefficient of $IONO_2$ has been calculated. This indicates that the photochemical lifetime of atmospheric $IONO_2$ is less than one minute under most sunlit conditions and consequently that photolysis is the main loss process for gaseous $IONO_2$. Thus, $IONO_2$ is thus not expected to act as a stable reservoir of atmospheric iodine during daytime.

The IONO₂ absorption cross-sections

J. C. Mössinger et al.

Title Page

Abstract	Introduction
Conclusions	References
Tables	Figures

◄◄   ►►

◄   ►

Back   Close

Full Screen / Esc

Print Version

Interactive Discussion

References

Atkinson, R., Baulch, D. J., Cox, R. A., Hampson, Jr., R. F., Kerr, J. A. and Troe, J.: Evaluated Kinetic and Photochemical Data for Atmospheric Chemistry, Supplement VIII, J. Phys. Chem. Ref. Data, 167–266, 2000.

Burkholder, J. B., Ravishankara, A. R., and Solomon, S.: Temperature-dependence of the $ClONO_2$ UV absorption spectrum, Geophys. Res. Lett., 21, 585–588, 1994.

Burkholder, J. B., Ravishankara, A. R., and Solomon, S.: UV visible and IR absorption cross-sections of $BrONO_2$, J. Geophys. Res., 100, 16 793–16 800, 1995.

Broske, R. and Zabel, F.: The UV-visible absorption spectrum of $IONO_2$, in Laboratory Experiments of Iodine Chemistry in the Stratosphere-LEXIS, EC, Brussels, 1998.

Chameides, W. L. and Davis, D. D.: Iodine: Its possible role in tropospheric photochemistry, J. Geophys. Res, 85, 7383–7393, 1980.

Chatfield, R. B. and Crutzen, P. J.: Are there interactions of iodine and sulfur species in marine air photochemistry, J. Geophys. Res, 95D, 22 319–22 341, 1990.

Curtis, A. R. and Sweetenham, W. P.: FACSIMILE, AERE Harwell publication R 12805, Computer Science and Systems Division, Harwell Laboratory, Oxfordshire, UK, 1987.

Davis, D., Crawford, J., Liu, S., McKeen, S., Bandy, A., Thornton, D., Rowland, F., and Blake, D.: Potential impact of iodine on tropospheric levels of ozone and other critical oxidants, J. Geophys. Res, 101, 2135–2147, 1996.

DeMore, W. B., Sander, S. P., Golden, D. M., Hampson, R. F., Kurylo, M. J., Howard, C. J., Ravishankara, A. R., Colb, C. E., and Molina, M. J.: Chemical Kinetics and Photochemical Data for use in Stratospheric Modeling, Evaluation No 12. Pasadena, CA, Jet Propulsion Laboratory, 1997.

Dillon, T.: Ph.D. thesis, University of Leeds, UK, 2001.

Gilles, M. K., Turnipseed, A. A., Talukdar, R. K., Rudich, Y., Villalte, P. W., Huey, L. G., Burkholder, J. B., and Ravishankara, A. R.: Reactions of O (P-3) with alkyl iodides: Rate coefficients and reaction products, J. Phys. Chem., 100, 14 005–14 015, 1996.

Holmes, N. S., Adams, J. W., and Crowley, J. N.: Uptake and reaction of HOI and $IONO_2$ on frozen and dry NaCl/NaBr surfaces and H_2SO_4, PCCP, 3, 1679–1687, 2001.

Jenkin, M. E.: The photochemistry of iodine containing compounds in the marine boundary layer, Technical Report AEA-EE-0405, Harwell Laboratory, Oxfordshire, UK, 1992.

Jenkin, M. E., Cox, R. A., and Candeland, D. E.: Photochemical aspect of tropospheric iodine

ACPD

2, 765–788, 2002

The IONO$_2$ absorption cross-sections

J. C. Mössinger et al.

Title Page

Abstract	Introduction
Conclusions	References
Tables	Figures

◀◀   ▶▶

◀   ▶

Back   Close

Full Screen / Esc

Print Version

Interactive Discussion

© EGS 2002

behaviour, J. Atmos. Chem., 2, 359–375, 1985.

McFiggans, G., Plane, J. M. C., Allan, B. J., Carpenter, L. J., Coe, H., and O'Dowd, C.: A modelling study of iodine chemistry in the marine boundary layer, J. Geophys. Res.-Atmos, 105, 14 363–14 369, 2000.

5 Plane, J. M. C.: Thermal decomposition of $IONO_2$, pers. commun., 2002.

Rowley, D. M., Harwood, M. H., Freshwater, R. A., and Jones, R. L.: A novel flash photolysis/UV absorption system employing charge-coupled device (CCD) detection: A study of the BrO + BrO reaction at 298 K, J. Phys. Chem., 100, 3020–3031, 1996.

Schmeisser, M. and Braendle, K.: Halogennitrate und ihre Reaktionen, Angew. Chem., 73,
10 388–393, 1961.

Turco, R. P., Toon, O. B., and Hamill, P.: Heterogeneous physicochemistry of the polar ozone hole, J. Geophys. Res., 94, 16 493–16 510, 1989.

Vogt, R., Sander, R., von Glasow, R., and Crutzen, P. J.: Iodine chemistry and its role in halogen activation and ozone loss in the marine boundary layer: A model study, J. Atmos. Chem., 32,
15 375–395, 1999.

The $IONO_2$ absorption cross-sections

J. C. Mössinger et al.

Title Page

Abstract	Introduction
Conclusions	References
Tables	Figures

⏮ ⏭

◀ ▶

Back Close

Full Screen / Esc

Print Version

Interactive Discussion

The IONO$_2$ absorption cross-sections

J. C. Mössinger et al.

Print Version

Interactive Discussion

Table 1. Concentrations used and generated during an experiment

	Before laser photolysis	After laser photolysis/ O atom reaction
N$_2$/ molecules cm^{-3}	2.5×10^{19}	2.5×10^{19}
NO$_2$/ molecules cm^{-3}	4.0×10^{15}	3.9×10^{15}
CF$_3$I/ molecules cm^{-3}	5.5×10^{16}	5.5×10^{16}
CF$_3$/ molecules cm^{-3}	–	7.5×10^{13}
IO/ molecules cm^{-3}	–	7.5×10^{13}
NO/ molecules cm^{-3}	–	8.5×10^{13}
NO$_3$/ molecules cm^{-3}	–	1.0×10^{12}

Table 2. Chemical reaction scheme used in the FACSIMILE model (Curtis and Sweetenham, 1987)

Reaction	Rate coeff. 295 K/cm^{-3} molecule^{-1} s^{-1}	Reference
$O(^3P) + NO_2 \rightarrow NO + O_2$	1.10×10^{-11}	(DeMore, et al., 1997)
$O(^3P) + NO_2 \rightarrow NO_3$	4.20×10^{-12}	(DeMore, et al., 1997)
$O(^3P) + CF_3I \rightarrow CF_3 + IO$	$1.10 \times 10^{-11}(*0.85)$	(Addison, et al., 1979)
$NO_2 + CF_3 \rightarrow CF_2O + FNO$	1.53×10^{-11}	(Pagsberg, et al., 1998)
$NO + CF_3 \rightarrow CF_3NO$	1.89×10^{-11}	(Ley, et al., 1995)
$CF_3 + CF_3 \rightarrow C_2F_6$	8.32×10^{-12}	(Rossi and Golden, 1979)
$IO + IO \rightarrow 2I + O_2$	$8.60 \times 10^{-11} (*0.7)$	(Bloss, et al., 2001)
$IO + IO \rightarrow OIO + I$	$8.60 \times 10^{-11} (*0.3)$	(Bloss, et al., 2001)
$O(^3P) + IO \rightarrow O_2 + I$	1.20×10^{-10}	(DeMore, et al., 1997)
$IO + NO_2 \rightarrow IONO_2$	9.00×10^{-12}	(DeMore, et al., 1997)
$I + NO_2 \rightarrow INO_2$	7.50×10^{-12}	(DeMore, et al., 1997)
$I + NO \rightarrow INO$	4.50×10^{-13}	(DeMore, et al., 1997)
$IO + NO \rightarrow I + NO_2$	2.20×10^{-11}	(DeMore, et al., 1997)
$I + INO_2 \rightarrow I_2 + NO_2$	8.32×10^{-11}	(v.d. Bergh and Troe, 1976)
$I + NO_3 \rightarrow IO + NO_2$	4.50×10^{-10}	(Chambers, et al., 1992)

Table 3. The absorption cross-sections of $IONO_2$ at 298 K

λ/nm	σ_{298}/molecule cm^{-2}
240	1.05×10^{-17}
245	1.40×10^{-17}
250	1.35×10^{-17}
255	1.19×10^{-17}
260	1.06×10^{-17}
265	9.85×10^{-18}
270	8.83×10^{-18}
275	8.54×10^{-18}
280	8.22×10^{-18}
285	7.71×10^{-18}
290	7.07×10^{-18}
295	6.47×10^{-18}
300	5.52×10^{-18}
305	5.16×10^{-18}
310	4.93×10^{-18}
315	4.83×10^{-18}
320	4.54×10^{-18}
325	4.46×10^{-18}

The IONO$_2$ absorption cross-sections

J. C. Mössinger et al.

© EGS 2002

Table 3. Continued...The absorption cross-sections of IONO$_2$ at 298 K

λ/nm	σ_{298}/molecule cm^{-2}
325	4.46×10^{-18}
330	4.29×10^{-18}
335	4.00×10^{-18}
340	3.86×10^{-18}
345	3.69×10^{-18}
350	3.52×10^{-18}
355	3.34×10^{-18}
360	3.13×10^{-18}
365	2.90×10^{-18}
370	2.64×10^{-18}
375	2.37×10^{-18}
380	2.10×10^{-18}
385	1.82×10^{-18}
390	1.58×10^{-18}
395	1.29×10^{-18}
400	1.02×10^{-18}
405	8.29×10^{-19}
410	6.95×10^{-19}
415	6.03×10^{-19}

Title Page

Abstract | Introduction

Conclusions | References

Tables | Figures

◄◄ | ►►

◄ | ►

Back | Close

Full Screen / Esc

Print Version

Interactive Discussion

© EGS 2002
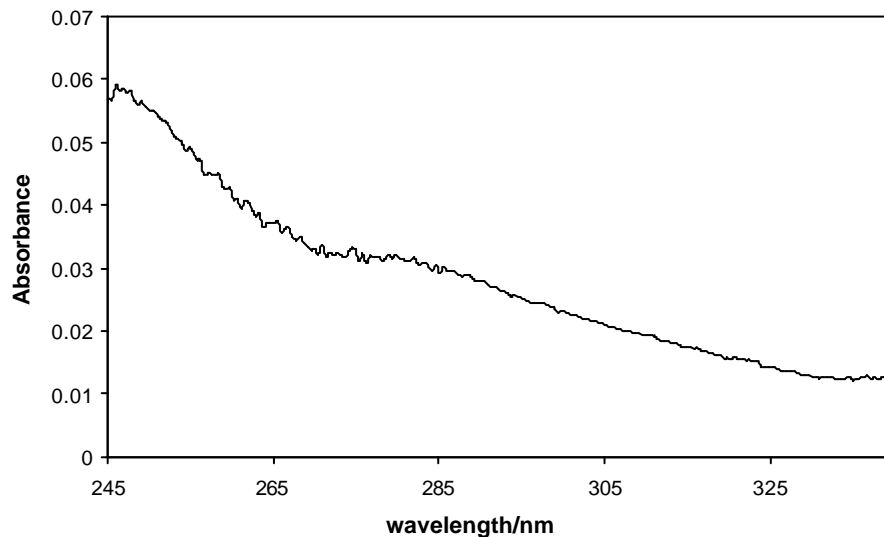
Fig. 1. Post flash absorption spectrum in the low wavelength region (245–340 nm) following flash photolysis of NO$_2$-CF$_3$I mixtures.

The IONO$_2$ absorption cross-sections

J. C. Mössinger et al.
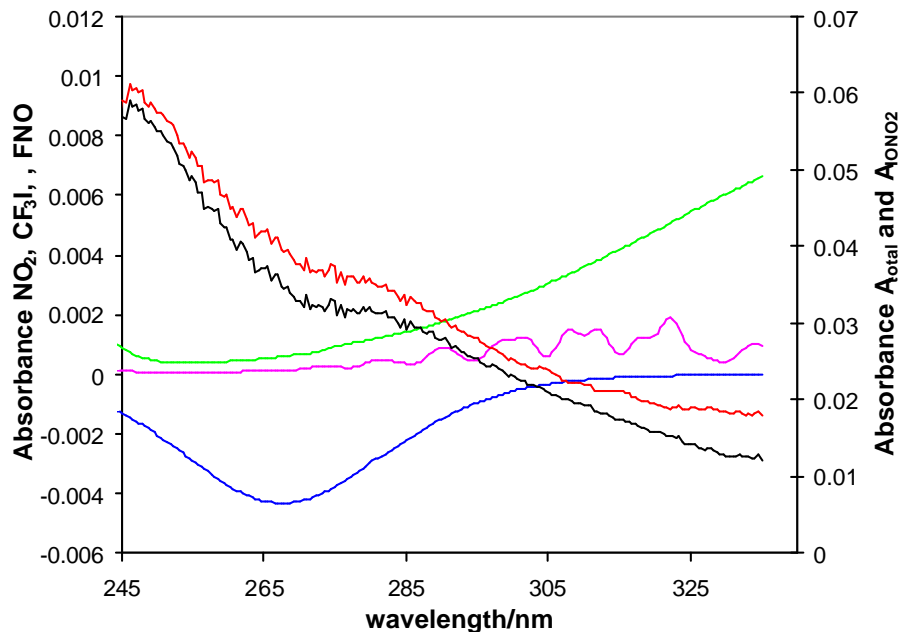
Fig. 2. Spectral stripping procedure in the low wavelength region (245–335 nm). Note changes in scale on the left and right hand axis. Black, pink, green and blue lines show the total absorption spectrum and absorption of FNO, NO$_2$, and CF$_3$I, respectively. The red spectrum is attributed to IONO$_2$ after the stripping procedure. The contribution of CF$_2$O is not shown as it only adsorbs below 245 nm.

**The IONO$_2$
absorption
cross-sections**

J. C. Mössinger et al.
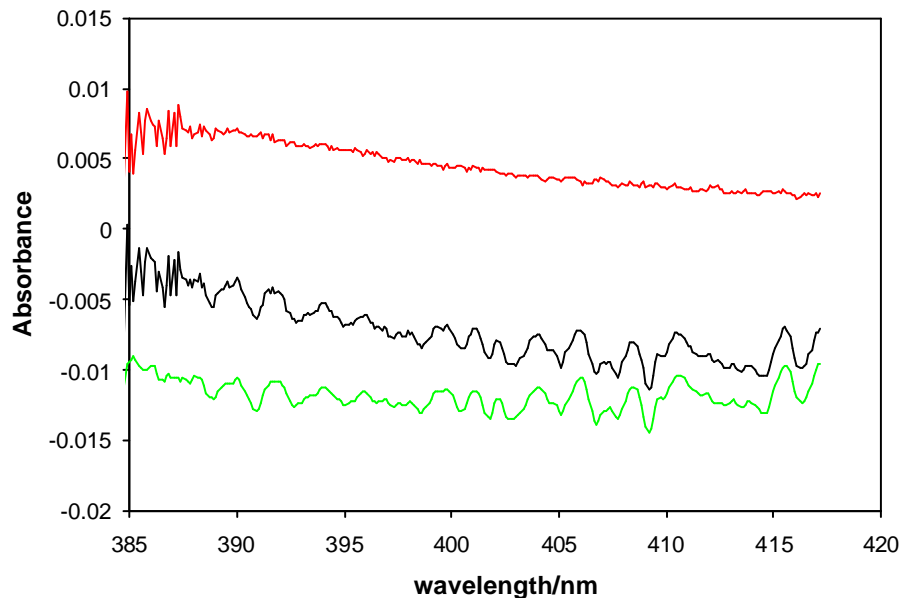
Fig. 3. Spectral stripping procedure in the high wavelength region (385–415 nm). Black, green and red lines show the total absorption spectrum, absorption of NO$_2$ and IONO$_2$ after the stripping procedure, respectively.
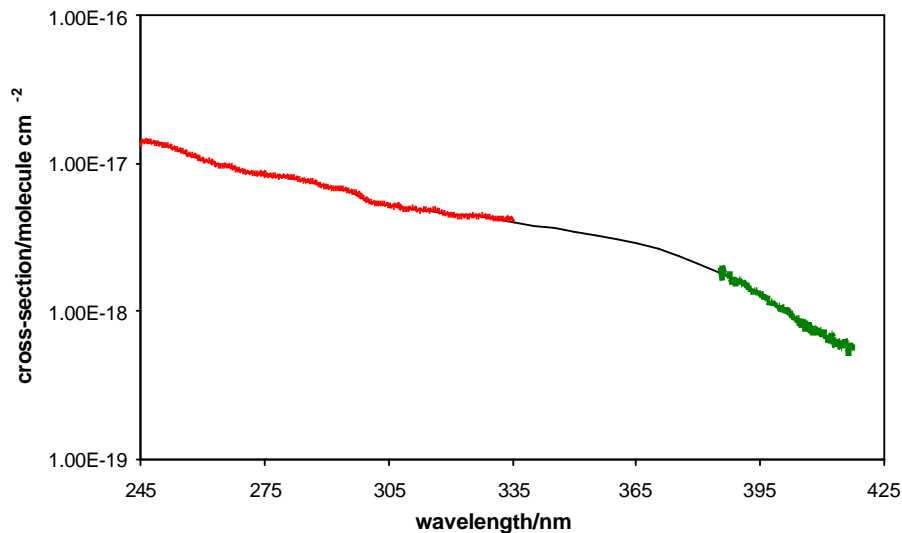
Fig. 4. Absorption spectrum of IONO$_2$. Red line: data recorded in the 245–335 nm region. Green line: data recorded in the 385–415 nm region. Black line: Fit to data.

Print Version

Interactive Discussion
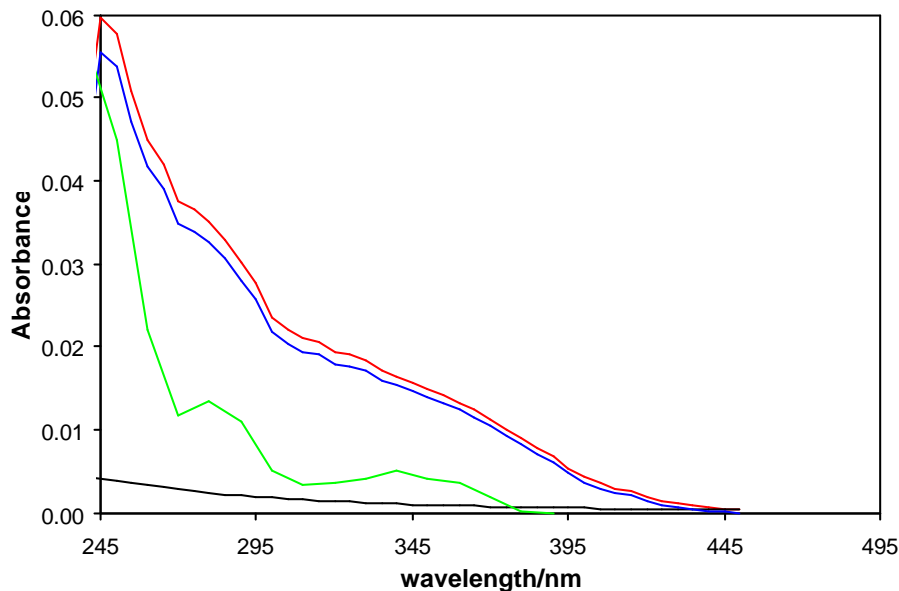
Fig. 5. Comparison of the absorption spectrum of IONO$_2$ (red), INO$_2$ (green) recorded by Broske and Zabel (1998) (scaled by using equal concentrations), the predicted absorption due to aerosol formation as a function of $1/\lambda^4$ (black) and the contribution due to aerosol absorption subtracted from the original absorption spectrum of IONO$_2$ (blue).

The IONO$_2$ absorption cross-sections

J. C. Mössinger et al.

© EGS 2002
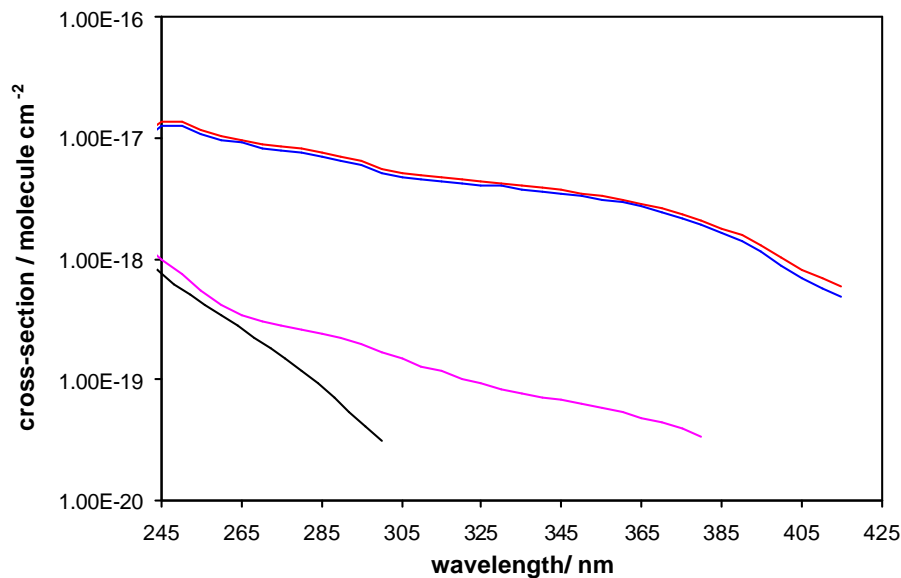
Fig. 6. Comparison of the absorption spectra of ClONO$_2$ (black), BrONO$_2$ (pink), IONO$_2$ (red) and (IONO$_2$-aerosol contribution) (blue).
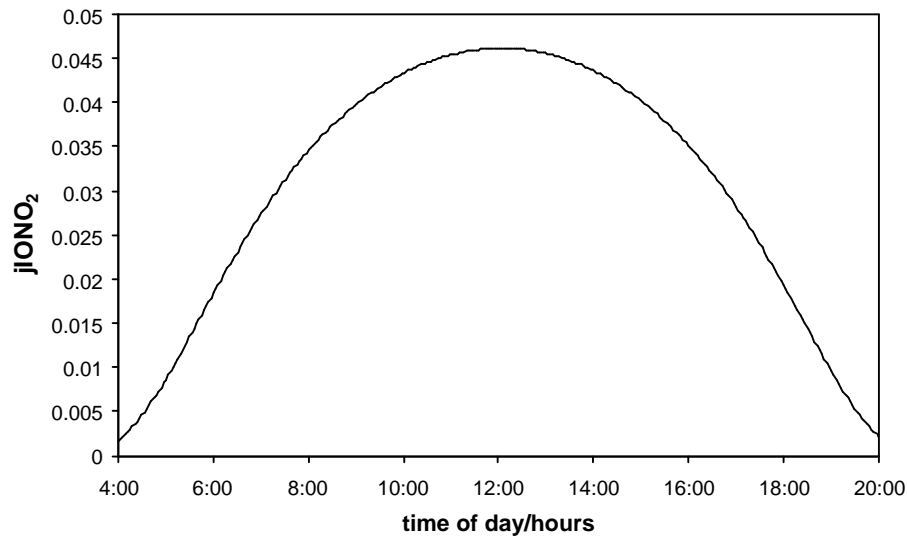
Fig. 7. J-values for IONO$_2$ as a function of time of day in the marine boundary layer, for midsummer 53° N (Mace Head, Ireland, July 1997).